Tunnelling resonances and Andreev reflection in transport of electrons through a normal-metal-quantum-dot-superconductor system

2002 J. Phys.: Condens. Matter 14 3641

(http://iopscience.iop.org/0953-8984/14/13/320)

INSTITUTE OF PHYSICS PUBLISHING JOURNAL OF PHYSICS: CONDENSED MATTER

J. Phys.: Condens. Matter **14** (2002) 3641–3651 PII: S0953-8984(02)31871-X

Tunnelling resonances and Andreev reflection in transport of electrons through a normal-metal–quantum-dot–superconductor system

Jin-Fu Feng[1,2] **and Shi-Jie Xiong**[1]

[1] National Laboratory of Solid State Microstructures and Department of Physics, Nanjing University, Nanjing 210093, People's Republic of China
[2] Department of Physics, Changshu College, Changshu 215500, People's Republic of China

Received 13 December 2001, in final form 25 February 2002
Published 22 March 2002
Online at stacks.iop.org/JPhysCM/14/3641

Abstract

The transport properties of electrons in a normal-metal–quantum-dot–superconductor system are investigated by the use of an equivalent single-particle multichannel network that takes into account the interaction of the dot and the pairing potential on the superconducting side. The transport properties depend on the interplay between the Coulomb blockade effect and Andreev reflection. It is found that at finite temperatures the conductance versus the gate voltage exhibits a series of peaks, due to the Andreev reflection, depending on the resonances controlled by the charging energy and level spacing of the dot. A detailed analysis of the physical origin of resonant peaks of different kinds is given.

1. Introduction

Owing to the advances in the nanotechnology, it is possible to investigate nanostructures in a tunable manner. Recently there has been much interest in transport properties of electrons in mesoscopic systems. In particular, those mesoscopic systems that consist of both normal parts and superconducting parts have been investigated intensively following the observation of several new phenomena related to the Andreev reflection [1–3]. More recently, several specific systems that include quantum dots as a part have introduced the possibility of observing new effects associated with the interplay between the superconducting pairing and the quantum-size effects of the dots. Due to the electron–electron interaction, the quantum dot (QD) can exhibit characteristic phenomena, e.g., the Coulomb blockade and Kondo effects. The tunnelling through a normal QD connected to superconducting leads, such as in superconductor–quantum-dot–superconductor (SDS) and normal-metal–quantum-dot–superconductor (NDS) structures, is found to possess special properties. As regards the NDS structures, Beenakker [4] presented a general multichannel S-matrix description and predicted resonant Andreev tunnelling for a single-level QD at the zero-bias limit. Later, Claughton *et al* [5] extended this theory to the

finite-bias case and found that differential conductance resonances are strongly suppressed in the weak-coupling limit. The Kondo anomaly in I–V curves in the presence of the Andreev reflection in the NDS system was discussed in [6,7]. The Andreev reflection in NDS systems with QD having multiple discrete levels was discussed using of a free-QD model, and resonant peaks of different kinds in the current versus gate voltage were discovered [8]. Very recently, Cuevas *et al* [9] investigated the transport properties of a QD coupled to a normal and a superconducting lead by means of the single-level Anderson model. Dolby *et al* [10] studied the effect of Coulomb interactions in the normal region of a normal–superconducting mesoscopic structure. In [11] and [12], Avishai *et al* calculated the I–V characteristics of electron tunnelling through an Anderson impurity between two superconductors and between a superconductor and a normal metal.

In this paper we investigate transport properties of electrons in the NDS system by the use of the equivalent single-particle multichannel network that takes into account the interaction on the dot and the pairing potential in the superconducting side. The present work, in contrast to [8] where the intradot Coulomb interactions are neglected and also [6,7,9,11] and [12] where only a single level of the QD is considered, studies the motion of electrons on the basis of many-body wavefunctions including all interacting electrons on the QD and one quasiparticle which tunnels through the dot. This method has been previously used to investigate the in-phase features of the transport of electrons through a dot in the Coulomb blockade regime with normal leads [13]. Here we assume that the QD has discrete multiple levels and the intradot Coulomb interaction is strong. We describe the pairing potential in the superconducting lead by the use of Bogoliubov–de Gennes Hamiltonian. The new results of the present study are as follows:

(i) A general formulation for the conductance of NDS systems is presented, taking into account the multilevel structure, the occupation status, the Coulomb interactions, the spin-flip scattering, and the Andreev reflection.

(ii) The dependence of the conductance, or the differential conductance, on the gate voltage, on the bias, and on the temperature, resulting from the combined effects of the physical ingredients mentioned above, is obtained.

(iii) It is found that at finite temperatures the conductance versus the gate voltage exhibits a series of peaks due to the Andreev reflection, depending on resonances controlled by the charging energy and level spacing of the dot.

(iv) The characteristics and the physical origin of resonant peaks of different kinds are analysed in detail.

The paper is organized as follows: in section 2 we describe the model and basic formalism; we present the calculated results in section 3; in the final section we give a brief summary and discussion.

2. The model and the basic formalism

The Hamiltonian of the system can be written as

$$H = H_N + H_D + H_S + H_T \tag{1}$$

where H_N, H_D, H_S, and H_S represent the normal wire, the QD, the superconducting wire, and the tunnelling between the dot and the leads, respectively. In a tight-binding scheme they can be written as

$$H_N = t_0 \sum_{\sigma,m<-1} (c^\dagger_{m,\sigma} c_{m+1,\sigma} + \text{H.c.}) + \sum_{\sigma,m\leqslant -1} \varepsilon_0 c^\dagger_{m,\sigma} c_{m,\sigma}, \tag{2}$$

$$H_D = \sum_{\sigma,i=1}^{N} (\xi_i + V_g) d^\dagger_{i,\sigma} d_{i,\sigma} + \frac{1}{2C}\left(e \sum_{i=1}^{N} \sum_{\sigma} d^\dagger_{i,\sigma} d_{i,\sigma} \right)^2, \tag{3}$$

$$H_S = t_0 \sum_{\sigma,m\geqslant 1} (c^\dagger_{m,\sigma} c_{m+1,\sigma} + \text{H.c.}) + \sum_{\sigma,m\geqslant 1} \varepsilon_0 c^\dagger_{m,\sigma} c_{m,\sigma} - \sum_{m\geqslant 1} (\Delta c^\dagger_{m,\uparrow} c^\dagger_{m,\downarrow} + \Delta^* c_{m,\downarrow} c_{m,\uparrow}) \tag{4}$$

$$H_T = \sum_{\sigma,i=1}^{N} (t^L c^\dagger_{-1,\sigma} d_{i,\sigma} + t^R c^\dagger_{1,\sigma} d_{i,\sigma} + \text{H.c.}) \tag{5}$$

where: $c_{m,\sigma}$ and $d_{i,\sigma}$ are annihilation operators for electrons in the leads and on the dot, with σ, m, and i being indices of spin, site, and level, respectively; t^L (t^R) is the matrix for the hopping between the left (right) lead and the dot which is assumed to be independent of the dot levels for simplicity; and N is the number of dot levels. The electron states on the close dot are characterized by the level energy ξ_i, dot potential V_g induced by the gate voltage, and charging energy of an effective capacitance C. In the left lead the motion of electrons is described by the site energy ε_0 and hopping integral t_0. In the right lead, Δ is the pairing potential of the Bogoliubov–de Gennes Hamiltonian for the superconductivity. In the following we set the site energy in the leads as the energy zero and choose t_0 as the energy unit.

Due to the superconductivity in the right lead, not only electrons, but also holes in the leads contribute to the conductance of the system. Both of them are considered as quasiparticles in the Fermi sea. We suppose that the dot has M electrons occupying levels below the chemical potential before and after tunnelling. Including one electron or one hole on the leads, there are in total $M \pm 1$ electrons in relevant many-body states. To solve the Schrödinger equation we use the following many-body wavefunctions as the basis [13]:

$$\Phi^{(e)}_{m,\sigma,D} = c^\dagger_{m\sigma}\left(\prod_{\{i\sigma'\}\in D} d^\dagger_{i\sigma'} \right)|F\rangle, \qquad \Phi_{D^{(+)}} = \left(\prod_{\{i\sigma'\}\in D^{(+)}} d^\dagger_{i\sigma'} \right)|F\rangle, \tag{6}$$

$$\Phi^{(h)}_{m,\sigma,D} = c_{m\sigma}\left(\prod_{\{i\sigma'\}\in D} d^\dagger_{i\sigma'} \right)|F\rangle, \qquad \Phi_{D^{(-)}} = \left(\prod_{\{i\sigma'\}\in D^{(-)}} d^\dagger_{i\sigma'} \right)|F\rangle, \tag{7}$$

where D, $D^{(+)}$, and $D^{(-)}$ denote sets of M, $M+1$, and $M-1$ states on the dot, respectively, and $|F\rangle$ represents the Fermi sea in the leads. A wavefunction that describes the tunnelling process can be written as a linear combination of these basis functions:

$$\Psi = \sum_{m,\sigma}\sum_{D} p^{(e)}_{m,\sigma,D}\Phi^{(e)}_{m,\sigma,D} + \sum_{D^{(+)}} q_{D^{(+)}}\Phi_{D^{(+)}} + \sum_{m,\sigma}\sum_{D} p^{(h)}_{m,\sigma,D}\Phi^{(h)}_{m,\sigma,D} + \sum_{D^{(+)}} q_{D^{(-)}}\Phi_{D^{(-)}}. \tag{8}$$

By applying the Hamiltonian to Ψ we obtain the following Schrödinger equations for the coefficients $p^{(e)}_{m,\sigma,D}$, $p^{(h)}_{m,\sigma,D}$, $q_{D^{(+)}}$, and $q_{D^{(-)}}$:

$$\chi_D p^{(e,h)}_{m,\sigma,D} \pm t_0(p^{(e,h)}_{m+1,\sigma,D} + p^{(e,h)}_{m-1,\sigma,D}) = E p^{(e,h)}_{m,\sigma,D}, \qquad (m < -1), \tag{9}$$

$$\chi_D p^{(e,h)}_{-1,\sigma,D} \pm t_0 p^{(e,h)}_{-2,\sigma,D} \pm \sum_i t^L q_{D^{(+,-)}(i,\sigma)} = E p^{(e,h)}_{-1,\sigma,D}, \tag{10}$$

$$\chi_{D^{(+,-)}(i,\sigma)} q_{D^{(+,-)}(i,\sigma)} \pm t^{L*} p^{(e,h)}_{-1,\sigma,D} \pm t^{R*} p^{(e,h)}_{1,\sigma,D} = E q_{D^{(+,-)}(i,\sigma)}, \tag{11}$$

$$\chi_D p^{(e)}_{1,\sigma,D} + t_0 p^{(e)}_{2,\sigma,D} + \sum_i t^R q_{D^{(+)}(i,\sigma)} + \Delta p^{(h)}_{1,-\sigma,D} = E p^{(e)}_{1,\sigma,D}, \tag{12}$$

$$\chi_D p^{(h)}_{1,\sigma,D} - t_0 p^{(h)}_{2,\sigma,D} - \sum_i t^R q_{D^{(-)}(i,\sigma)} + \Delta^* p^{(e)}_{1,-\sigma,D} = E p^{(h)}_{1,\sigma,D}, \tag{13}$$

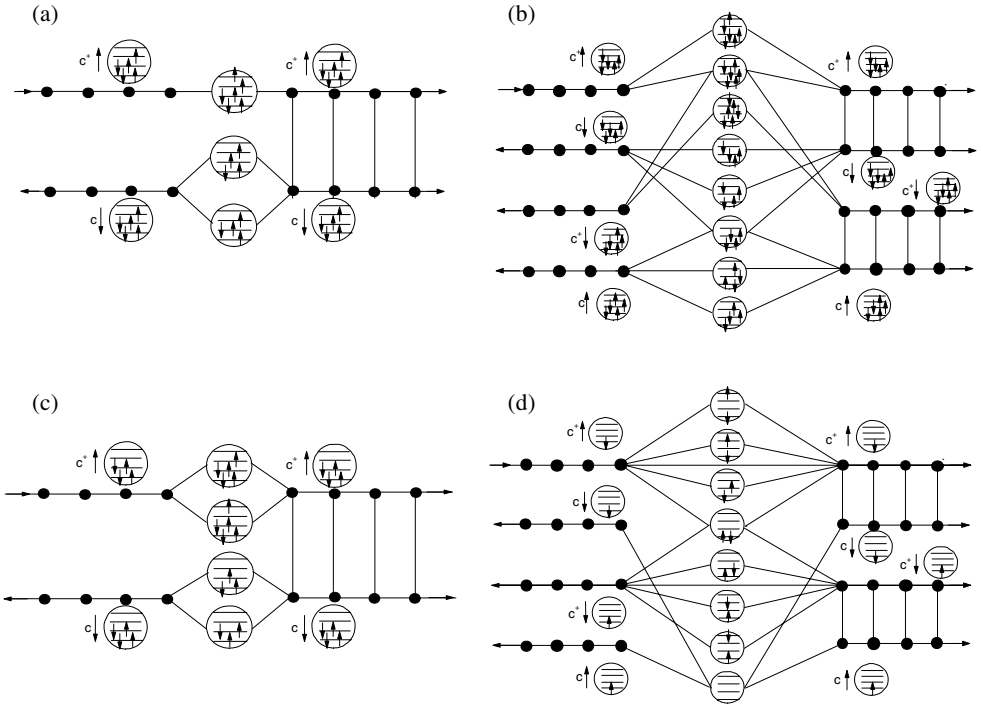

Figure 1. Illustrations of the equivalent single-particle networks for electron tunnelling through a NDS system. Four energy levels on the dots are included. The lead is described with a one-dimensional tight-binding lattice. There are five electrons on the dot for (*a*) and (*b*), four electrons for (*c*), and one electron for (*d*), before and after tunnelling. The states on the dot are shown in circles. The position and spin of the tunnelling electron are represented by the lattice sites and ↑ or ↓ signs, respectively. $c^{\dagger}$ (c) stands for electron (hole) channels.

$$\chi_D p^{(e)}_{m,\sigma,D} + t_0(p^{(e)}_{m+1,\sigma,D} + p^{(e)}_{m-1,\sigma,D}) + \Delta p^{(h)}_{m,\sigma,D} = E p^{(e)}_{m,\sigma,D}, \qquad (m > 1), \tag{14}$$

$$\chi_D p^{(h)}_{m,\sigma,D} - t_0(p^{(h)}_{m+1,\sigma,D} + p^{(h)}_{m-1,\sigma,D}) + \Delta^* p^{(e)}_{m,-\sigma,D} = E p^{(h)}_{m,\sigma,D}, \qquad (m > 1), \tag{15}$$

where E is the total energy of the $M + 1$ particles, $D^{(+)}(i,\sigma)$ ($D^{(-)}(i,\sigma)$) is the set of dot states obtained from D by adding (subtracting) state $\{i\sigma\}$, the sum on i is over all possible sets $D^{(+)}(i,\sigma)$ ($D^{(-)}(i,\sigma)$), and

$$\chi_D = \frac{e^2M^2}{2C} + MV_g + \sum_{i\in D}\xi_i \tag{16}$$

$$\chi_{D^{(+,-)}(i,\sigma)} = \frac{e^2(M \pm 1)^2}{2C} + (M \pm 1)V_g + \sum_{i\in D^{(+,-)}(i,\sigma)}\xi_i. \tag{17}$$

In the following calculation we will include four discrete levels with equal level spacing for the dot. From these equations the problem of the transmission through the NDS system reduces to a single-particle picture of a multichannel network. In figures 1(*a*) and (*b*) we partially show possible networks for a dot with five (an odd number of) electrons before and after tunnelling. The symbols $c^{\dagger}$ and c denote the electron and hole channels in the leads, respectively. The states of the dot are represented by the occupation statuses of the levels shown in the circles. To keep the current steady, the outgoing channels should have the same status of level occupation as the incoming channel. However, the spin of the electron on the

dot may be flipped. Figure 1(*b*) shows the spin-flip process in the tunnelling. In figure 1(*c*) we display the tunnelling process in the case of an even number of electrons on a dot. In the intermediate states the tunnelling electron goes to empty levels, while the hole from the superconducting side goes to an occupied level, creating a Cooper pair on the superconducting lead. In figure 1(*d*) we show the tunnelling process with only one electron on the dot. There are other independent networks which are not shown.

If an electronic plane wave with unit amplitude is incident from the left (normal) lead, in both electron and hole channels of the left lead there are reflected waves, and the coefficients $p^{(e,h)}_{m,\sigma,D}$ can be written as

$$p^{(e)}_{m,\sigma,D} = \mathrm{e}^{\mathrm{i}k^{(e)}m} + r^{(e)}_{\sigma,D}\mathrm{e}^{-\mathrm{i}k^{(e)}m}, \qquad \text{for } m < 0, \tag{18}$$

$$p^{(h)}_{m,\sigma,D} = r^{(h)}_{\sigma,D}\mathrm{e}^{-\mathrm{i}k^{(h)}m}, \qquad \text{for } m < 0, \tag{19}$$

where $r^{e,h}_{\sigma,D}$ and $k^{(e,h)}$ are, respectively, the reflection amplitude and wavevector in the corresponding channel. The wavevectors satisfy $\epsilon = 2t_0 \cos k^{(e)} + \epsilon_0 - eV_b$ and $\epsilon = -2t_0 \cos(-k^{(h)}) - \epsilon_0 + eV_b$, where $\epsilon = E - \chi_D$ is the energy of the tunnelling particle and V_b is the bias voltage. We can calculate the reflection amplitudes $r^{(e,h)}_{\sigma,D}$ for all channels in network l by solving the above Schrödinger equations. By virtue of current conservation, at low temperature and bias voltage the current can be evaluated in the normal region and can be expressed as [14, 15]

$$I(V_b) = \frac{2e^2}{h}\int_{-\infty}^{\infty} \mathrm{d}\epsilon \sum_l [f_0(\epsilon - eV_b) - f_0(\epsilon)]F_l(T)[N^{(e)}_l - \mathrm{Tr}(\hat{R}^{(e)\dagger}_l \hat{R}^{(e)}_l) + \mathrm{Tr}(\hat{R}^{(h)\dagger}_l \hat{R}^{(h)}_l)] \tag{20}$$

where $\hat{R}^{(e)}_l$ and $\hat{R}^{(h)}_l$ are reflection matrices for, respectively, electron and hole channels on the normal side of network l, $N^{(e)}_l$ is the number of electron channels in network l, $f_0(\epsilon, T)$ is the Fermi distribution of electrons in the normal lead, and $F_l(T)$ is the thermal probability of the dot state in network l:

$$F_l(T) = \frac{1}{\mathcal{N}} \exp\left(-\frac{\chi_{D_l}}{k_B T}\right) \qquad \text{with } \mathcal{N} = \sum_{\{D\}} \exp\left(-\frac{\chi_D}{k_B T}\right), \tag{21}$$

with χ_{D_l} being energy of the dot state corresponding to network l. The contribution of Andreev reflection to the conductance is included by $\hat{R}^{(h)}_l$ in equation (20). By sweeping the gate voltage V_g, the occupation number of the dot is sequentially changed, corresponding to a series of resonant conductance peaks. The spacing between peaks is determined by both the charging energy and the level spacing.

3. Results and discussion

On the basis of the set of Schrödinger equations, we carry out numerical calculations of the transport properties of the NDS system. In the case of $|\epsilon| < \Delta$, only the Andreev reflection makes a contribution to the current. Figure 2(*a*) presents the current I as a function of the gate voltage V_g at small bias voltage. A series of peaks emerge in the I–V_g curve. In the regime of Coulomb blockade, these peaks correspond to resonances with different numbers of electrons on the dot. There are two types of peak, A-type and B-type, present alternately in the series, as shown in the figure. The latter is more strongly dependent on the bias voltage. A-type peaks originate from the Andreev reflection in the case with an odd number of electrons on the dot, corresponding to the processes shown in figures 1(*a*) and (*b*). The B-type peaks result from resonances in the case of an even number of electrons on the dot, as shown in figure 1(*c*).

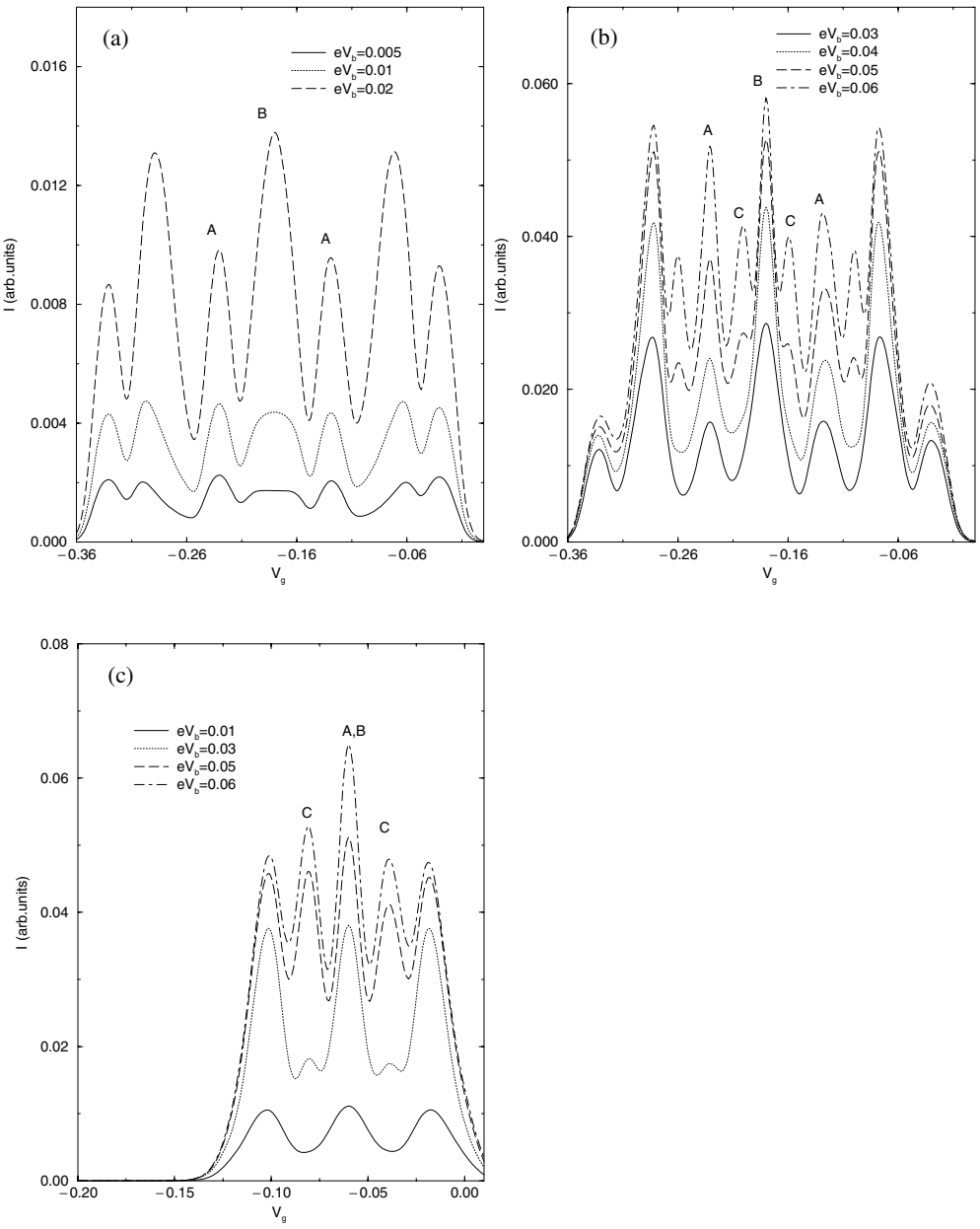

Figure 2. Current I as a function of gate voltage V_g. The energy unit is t_0. The parameters are chosen as $\Delta = 0.15$, $t^L = t^R = 0.1$, $k_BT = 0.005$, and the level spacing is 0.04. For (a) and (b) the charging energy $e^2/2C = 0.015$. For (c) $e^2/2C = 0$.

In this case the tunnelling electron goes to an empty level of the dot, then creates a Cooper pair on the superconducting side by Andreev reflecting a hole in an occupied level of the dot. At low temperatures the main contributions to the current come from the intermediate dot states situated in energy window $[\epsilon_F - eV_b, \epsilon_F]$ with ϵ_F the Fermi energy in the lead, as can be seen from equation (20). For the A-type peaks, only one level on the dot is involved in the resonant tunnelling: the electron from the normal lead goes to the singly occupied level of the dot to

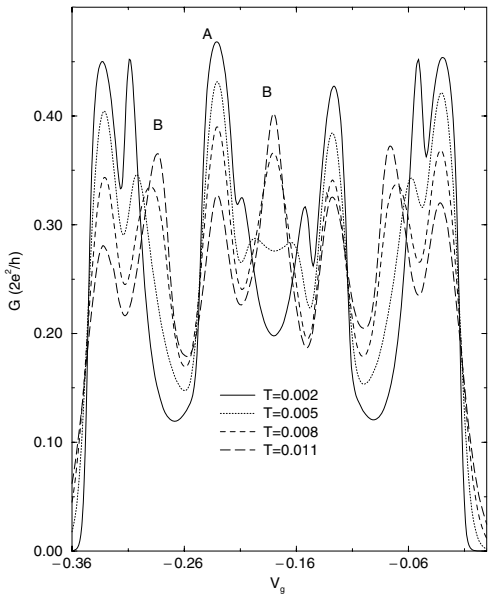

Figure 3. Linear conductance G versus gate voltage V_g at different temperatures. The temperature unit is t_0/k_B. The parameters are chosen as $\Delta = 0.15$, $t^L = t^R = 0.1$, $e^2/2C = 0.015$, and the level spacing is 0.04.

form a Cooper pair entering the superconducting lead by reflecting a hole to the normal lead, leaving this level remaining singly occupied. Thus, the A-type resonant tunnelling can occur at very low temperatures and low bias, provided that the Fermi level of the lead coincides with a level of the dot which is singly occupied. In contrast, for the B-type tunnelling at least two levels of the dot should be involved: one is originally empty—for accommodating the electron from the normal lead—and the other is doubly occupied—for receiving a hole from the superconducting lead in the Andreev reflection. As a result, the B-type tunnelling can occur only at finite temperatures, or at zero temperature but with a finite bias to form an energy window including these two levels. This is why the B-type peaks are more strongly dependent on the value of the bias. The A-type peaks (corresponding to even occupations of the dot) and B-type peaks (odd occupations) appear alternately when varying the gate voltage, and the spacing between adjacent A-type and B-type peaks is determined by both the charging energy and the level spacing. In the case with thermal energy and bias less than the level spacing or the charging energy, each of these peaks corresponds to one occupation status (including the occupation number and the levels used for the intermediate states). However, if the temperature is higher or the bias is comparable to the level spacing or the charging energy, a new type of peak may appear due to contributions from states with different occupation number or different levels used. This is demonstrated by the C-type peaks in figure 2(b) which appear between A-type and B-type peaks at relatively larger bias voltage. The complicated peak structure reflects the coexistence of two parameters (charging energy and level spacing) that control the resonant tunnelling. For comparison, the I–V_g curves of the non-interacting case are shown in figure 2(c). In this case the peak structure is much simpler even for relatively large bias. The A-type and B-type peaks merge together due to the spin degeneracy of the dot levels that erases the difference in energy of intermediate states between even and odd occupation. At relatively larger bias the C-type peaks also appear due to the tunnelling through different dot levels.

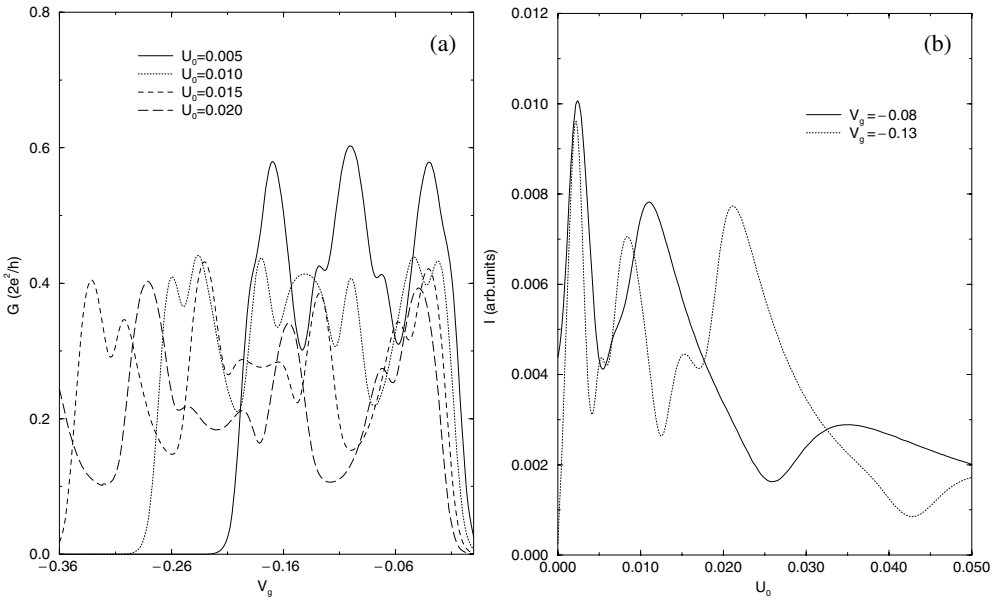

Figure 4. (*a*) The linear conductance as a function of gate voltage at different U_0. (*b*) The current versus U_0 at $eV_b = 0.01$. The other parameters are $\Delta = 0.15$, $t^L = t^R = 0.1$, $k_BT = 0.005$, and the level spacing is 0.04.

We also calculate the linear conductance as a function of gate voltage. In figure 3 we plot the linear conductance versus gate voltage at different temperatures. It can be seen that the B-type conductance peaks are strongly suppressed at low temperatures and the C-type peaks disappear, since at zero bias the tunnelling process involving more than one level can occur only via the thermal excitations. At very low temperature (the solid curve), each of the A-type peaks is split into two peaks. This is due to the difference in the resonant energy between the non-spin-flip (figure 1(*a*)) and spin-flip (figure 1(*b*)) tunnelling processes in the case of odd occupations of the dot. When the temperature increases this difference is erased by the thermal excitations and the two peaks merge together.

Figure 4(*a*) shows the conductance versus gate voltage for different U_0 ($\equiv e^2/2C$). With increasing U_0, the peak structure becomes more complicated. This is partially due to the separation of the A-type and B-type peaks which merge together at zero U_0, and partially due to the splitting of the A-type peaks caused by the many-body effect on the dot. In figure 4(*b*) we plot the current as a function of charging energy $e^2/2C$ at different gate voltages V_g. As one can see, despite the oscillations from sweeping through the resonances, the increase of the charging energy leads to the ceasing of the Andreev transport (Coulomb blockade). It has been shown that the electron–electron interaction can cause suppression of Andreev reflection due to the orthogonality catastrophe [16, 17].

Figures 5(*a*) and (*b*) show the differential conductance as a function of the bias voltage for different temperatures at $V_g = -0.18$ and -0.02, respectively. As expected, in both figures the peak structure is smoothed by increasing the temperature due to the thermal excitations. The number and positions of peaks are different in figures 5(*a*) and (*b*). In the case of $V_g = -0.18$, there are four electrons on the dot occupying two levels, as shown in figure 1(*c*). For $V_g = -0.02$, there is only one electron on the dot and the process of Andreev reflection is illustrated in figure 1(*d*). The number of intermediate states in figure 1(*d*) is much larger than that of 1(*c*). This causes denser peaks in figure 5(*b*).

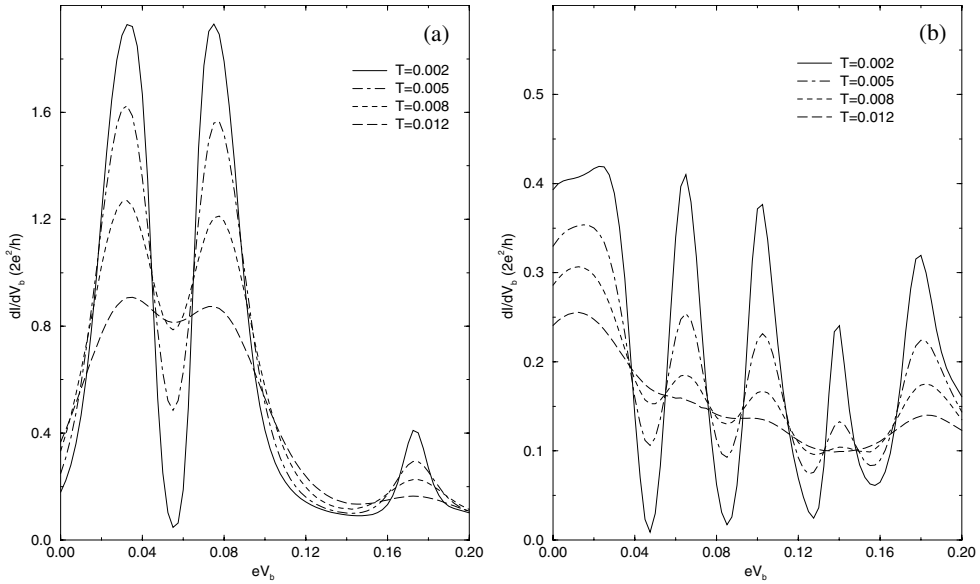

Figure 5. The differential conductance versus eV_b at different temperatures. (a) and (b) correspond to gate voltages of $V_g = -0.18$ and -0.02, respectively. The other parameters are chosen as $\Delta = 0.15$, $t^L = t^R = 0.1$, $e^2/2C = 0.015$, and the level spacing is 0.04.

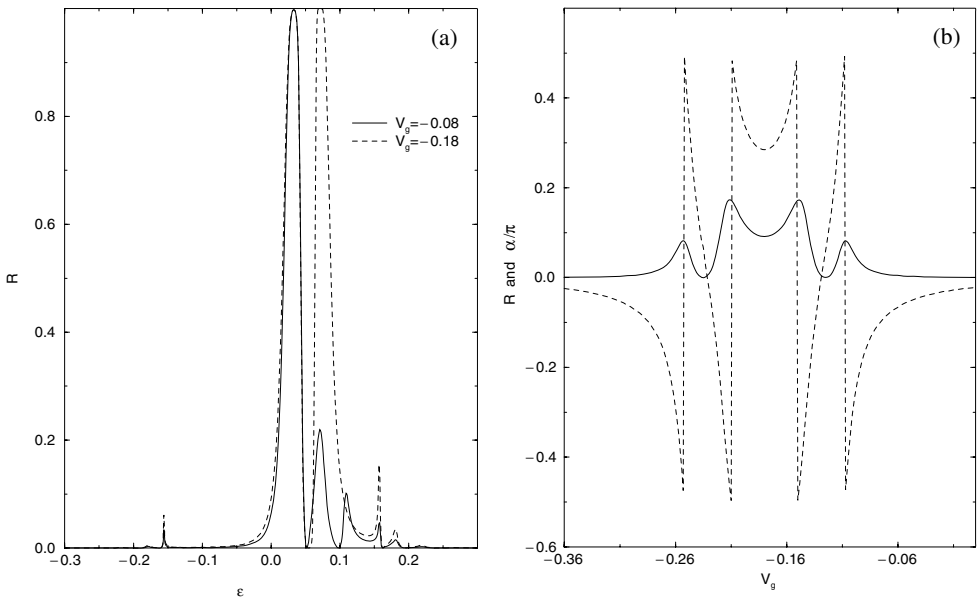

Figure 6. (a) The total probability of Andreev reflection R as a function of electron energy ϵ. (b) The magnitude R (solid curve) and phase α (dashed curve) of Andreev reflection in the hole channel of figure 1(c) as functions of V_g. The parameters are $e^2/2C = 0.015$, $t^L = t^R = 0.1$, $\Delta = 0.15$.

In figure 6(a) we display the dependence of the total tunnelling probability on electron energy ϵ. The peaks in the curves reflect the resonances $\xi_{D^{(+,-)}(i,\sigma)}$ for Andreev reflection through the dot. The peak number in the case of $V_g = -0.08$ is larger than that in the

case of $V_g = -0.18$, owing to the larger number of resonance levels. Note that in the case of symmetric barriers ($t^L = t^R$), the probability of the resonance Andreev reflection is of the order of unity, much larger than that of the non-resonant Andreev reflection of the normal–superconducting junctions with a single barrier. This is consistent with results obtained in [8]. It is also interesting to investigate the variation of the phase in the Andreev reflection. In figure 6(b) we show the magnitude and phase of the Andreev reflection amplitude $r^{(h)}$, corresponding to a network with one hole channel shown in figure 1(c), as functions of the dot potential V_g. As one can see, the phase changes abruptly by π at every resonant peak of Andreev reflection, and it varies continuously between the resonant peaks. Thus, the phase of the Andreev reflection can be controlled by the gate voltage in such a structure.

4. Summary

We have investigated the electronic transport through a QD coupled to normal and superconducting leads on either side by using the equivalent multichannel network method. We consider both the multiple levels and the Coulomb interaction on the dot. In this system the tunnelling current measured in the normal lead arises mainly from contributions from the Andreev reflection. The results obtained show that

(i) both the intensity and the phase of the Andreev reflection are controlled by the resonant tunnelling through the dot which can be tuned by varying the gate voltage;
(ii) for even occupation of the dot the resonant tunnelling involves two dot levels, one for the electron and the other for the hole;
(iii) the tunnelling spectrum depends on both Coulomb interaction and level spacing of the dot; their combined effect leads to complicated structures of peaks;
(iv) the magnitude of the resonant Andreev reflection in this system may be much larger than that in the usual normal–superconducting junction with a single barrier.

In this paper the resonant conditions for resonant Andreev reflection are discussed. We have also shown that the strong electron–electron interactions suppress the conductance of the system.

Acknowledgments

This work was supported by National Foundation of Natural Science in China Grants Nos 69876020 and 10074029, and by the China State Key Projects of Basic Research (G20000683).

References

[1] Hurd M, Löfwander T, Johansson G and Wendin G 1999 *Phys. Rev.* B **59** 4412
[2] Fitzgerald R J, Pohlen S L and Tinkham M 1998 *Phys. Rev.* B **57** R11 073
[3] De Jong M J M and Beenakker C W J 1995 *Phys. Rev. Lett.* **74** 1657
[4] Beenakker C W J 1992 *Phys. Rev.* B **46** 12 841
[5] Claughton N R, Leadbeater M and Lambert C J 1995 *J. Phys.: Condens. Matter* **7** 8757
[6] Fazio R and Raimondi 1998 *Phys. Rev. Lett.* **80** 2913
[7] Kang K 1998 *Phys. Rev.* B **58** 9641
[8] Sun Q F, Wang J and Lin T H 1999 *Phys. Rev.* B **59** 3831

[9] Cuevas J C, Yeyati A L and Martín-Rodero A 2001 *Phys. Rev.* B **63** 094515
[10] Dolby P, Seviour R and Lambert C J 2001 *J. Phys.: Condens. Matter* **13** L147
[11] Avishai Y, Golub A and Zaikin A D 2001 *Phys. Rev.* B **63** 134515
[12] Avishai Y, Golub A and Zaikin A D 2001 *Europhys. Lett.* **54** 640
[13] Xiong S J and Xiong Y 1999 *Phys. Rev. Lett.* **83** 1407
[14] Takagaki Y 1998 *Phys. Rev.* B **57** 4009
[15] Strijkers G J, Ji Y, Yang F Y and Chien C L 2001 *Phys. Rev.* B **63** 104510
[16] Kinaret J M, Meir Y, Wingreen N S, Lee P A and Wen Xiao-Gang 1992 *Phys. Rev.* B **46** 4681
[17] Matveev K A, Glazman L I and Baranger H U 1996 *Phys. Rev.* B **53** 1034